Dependent modal space control

2013 Smart Mater. Struct. 22 105004

(http://iopscience.iop.org/0964-1726/22/10/105004)

IOP Publishing Smart Materials and Structures
Smart Mater. Struct. **22** (2013) 105004 (11pp) doi:10.1088/0964-1726/22/10/105004

Dependent modal space control

M Serra, F Resta and F Ripamonti

Politecnico di Milano, Mechanical Engineering Department, Via La Masa, 1 Milano, Italy

E-mail: mattiaserra27@gmail.com and francesco.ripamonti@polimi.it

Received 24 April 2013, in final form 25 July 2013
Published 29 August 2013
Online at stacks.iop.org/SMS/22/105004

Abstract
This paper presents a new control technique for reducing vibration in flexible structures. It is based on the modal approach and is called dependent modal space control (DMSC). The well-known independent modal space control (IMSC) method, devised in the 1980s, allows the frequency and damping of the controlled modes to be changed using diagonal control gain matrices, leaving the mode shapes unaltered. DMSC, on the other hand, can impose not only frequency and damping but also the controlled mode shapes by using full control gain matrices. In many applications, owing to the limited number of sensors–actuators available for control and the increasing spillover effects, generic assignment of eigenvectors is not possible.

However, an optimal eigenstructure assignment can be computed to reduce structure vibration by minimizing an input–output performance index. To demonstrate the advantages of this new method, we compare IMSC and DMSC using numerical simulation on a finite element method model of a cantilevered beam.

(Some figures may appear in colour only in the online journal)

1. Introduction

In recent years, vibration control has become increasingly important, and as a result much effort has been put into studying it. This is because light and flexible structures generally have a low damping ratio, especially on the first modes, which in many applications are also the most excited. These vibrations cause fatigue problems or simply downgrade performance beyond the acceptable thresholds in precision applications.

Among the various vibration control strategies, one of the most used is modal control. It was introduced by Balas [1] and Meirovitch [2] between the 1970s and 1980s. It permits control of continuum structures with infinite degrees of freedom using a reduced order model with few degrees of freedom (dofs) thanks to a change of the variables in the principal coordinates. In addition, unlike other control logics, the modal method has a well defined physical meaning in the gain matrix definition. A few years after the introduction of modal control, Meirovitch proposed independent modal space control (IMSC), which uses a modal filter to estimate the modal states needed by the control law [3]. Starting from the original IMSC, many improvements were developed to improve its performance and reduce the effects of control and observation spillover [4, 5]. An example of these improvements came from Baz and Poh [6] and then Fang, Li and Jeary [7], who developed modified independent modal space control using some of the weighting matrix entries of the LQR method. A further improvement of modified independent modal space control (MIMSC) came from Singh and Agarwal [8]. In their approach, the energy of different modes is checked at specific intervals of time and the main control effort is directed towards the dominant modes. Kim and Inman [9] developed a sliding mode observer in order to eliminate observation spillover, improving the performance of IMSC and ensuring higher robustness in the control method.

It is important to note that all these methods make it possible to modify frequencies and damping ratios of the controlled modes independently, without affecting the system mode shapes, by using a diagonal gain matrix for the principal coordinates.

Other kinds of control logic exist; for example, the pole–zero assignment method [10], which is not model based, requires collocated sensors and actuators and allows zeros and poles of the determined frequency response function (FRF) to be imposed in a closed loop. This kind of control strategy has many limitations, and is very different from those illustrated above.

This paper presents a strategy for assigning the controlled eigenvalues and eigenvectors desired (as a linear combination

of those not controlled), while also exploiting the non-diagonal entries of the controller matrix. In other words, in terms of the available control parameters, some of the coefficients of the gain matrix are used to assign the closed loop poles, while the remaining ones are used to impose the eigenvectors. In the case of distributed sensors–actuators, thus without spillover, it is possible, for example, to create virtual nodes in desired locations of the controlled modes using the eigenstructure assignment, with great advantages in many applications.

Nevertheless, most control problems have a very limited number of actuators and sensors, and this result cannot be obtained. In these cases, mode shape assignments are computed by minimizing a desired performance index, e.g. the integral of the magnitude of the FRF, between a disturbance input and a desired output in a given frequency range. The minimization problem is constrained in order to ensure the stability of the closed loop system on a set of modes that can be different from the number of controlled ones, allowing the index to consider only the absolute value of the FRF and disregard phase. Since the performance index derives from an input–output relation, this method requires that the position of the disturbance or its Lagrangian components be known.

The proposed algorithm ensures internal stability, avoiding problems of zero–pole cancellations within the limits of the number of modes selected for inclusion in the optimization procedure. The number of modes used is a control design decision and must be made balancing performance index accuracy against the work needed to identify the system parameters. The name dependent modal space control emphasizes the differences between the logic proposed, which couples the uncontrolled modes, and IMSC, where the modes also remain uncoupled in the closed loop.

In this paper, to demonstrate the performance of the method, a clamped beam was controlled with three actuators and three accelerometers in the most general non-collocated configuration. Numerical simulations were carried out and the differences between IMSC and dependent modal space control (DMSC) are presented, focusing also on actuation, observation and stability issues.

2. The eigenstructure assignment problem

This section presents an analytical method for assigning eigenvalues and eigenvectors in a linear time invariant system. For simplicity, a simple two dof discrete system (figure 1) is used to illustrate the procedure. The same algorithm is valid for systems of a higher dimension without loss of generality. Note that this procedure of eigenstructure assignment has some restrictions due to its application in the mechanical field, and is different from a more general eigenstructure assignment procedure described for instance in [11, 12]. Consider the system's equations of motion

$$[\mathbf{M}]\,\underline{\ddot{\mathbf{z}}} + [\mathbf{R}]\,\underline{\dot{\mathbf{z}}} + [\mathbf{K}]\,\underline{\mathbf{z}} = [\mathbf{\Lambda_{F_c}}]^{\mathbf{T}}\underline{\mathbf{F_c}} + [\mathbf{\Lambda_{F_d}}]^{\mathbf{T}}\underline{\mathbf{F_d}} \qquad (1)$$

where $[\mathbf{M}]$, $[\mathbf{R}]$, $[\mathbf{K}]$ are the inertial, damping and stiffness matrices, the vector $\underline{\mathbf{z}}$ contains the independent variables in physical coordinates, the matrices $\left[\mathbf{\Lambda_{F_c}}\right]^{\mathbf{T}}$ and $\left[\mathbf{\Lambda_{F_d}}\right]^{\mathbf{T}}$ link

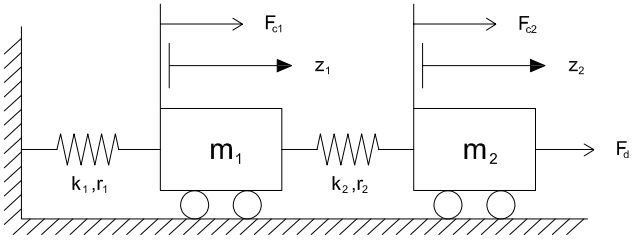

Figure 1. A discrete two dof system.

the location of application of the forces with the independent variables and $[\mathbf{F_c}]$, $[\mathbf{F_d}]$ are respectively the control forces and the disturbance acting on the system. To implement the control logic and write the closed loop matrices, the disturbance force does not need to be considered and will be omitted below. From equation (1), it is possible to build the state space form as

$$\underline{\dot{\mathbf{x}}} = [\mathbf{A}]\,\underline{\mathbf{x}} + [\mathbf{B_c}]\,\underline{\mathbf{F_c}} \qquad (2)$$

where

$$\begin{aligned} \underline{\mathbf{x}} &= \begin{bmatrix} \underline{\dot{\mathbf{z}}} \\ \underline{\mathbf{z}} \end{bmatrix} \\ [\mathbf{A}] &= \begin{bmatrix} -[\mathbf{M}]^{-1}[\mathbf{R}] & -[\mathbf{M}]^{-1}[\mathbf{K}] \\ [\mathbf{I}] & [\mathbf{0}] \end{bmatrix} \\ [\mathbf{B_c}] &= \begin{bmatrix} [\mathbf{M}]^{-1}[\mathbf{\Lambda_{F_c}}]^{\mathbf{T}} \\ [\mathbf{0}] \end{bmatrix} \\ \underline{\mathbf{F_c}} &= \begin{bmatrix} F_{c1} \\ F_{c2} \end{bmatrix}. \end{aligned} \qquad (3)$$

Considering the state feedback structure, from the expression of the control input

$$\underline{\mathbf{F_c}} = [\mathbf{G}]\underline{\mathbf{x}} \qquad (4)$$

where $[\mathbf{G}]$ is the control gain matrix, it is possible to compute the closed loop state matrix

$$[\mathbf{A_{cl}}] = [\mathbf{A}] + [\mathbf{B_c}][\mathbf{G}]. \qquad (5)$$

Looking at the $[\mathbf{B_c}]$ matrix due to the state space formulation, it is possible to see that the closed loop dynamic matrix will change only in the first half of the rows. As a consequence, considering the structure of $[\mathbf{A_{cl}}]$, it is clear that the terms modified by the control law are the entries in the first two rows. Writing the closed loop matrix in a generic way

$$\left[\mathbf{A_{cl}}\right] = \begin{bmatrix} a_{11} & a_{12} & a_{13} & a_{14} \\ a_{21} & a_{22} & a_{23} & a_{24} \\ 1 & 0 & 0 & 0 \\ 0 & 1 & 0 & 0 \end{bmatrix} \qquad (6)$$

the target for the control law is to find the eight coefficients a_{ij} in order to assign the eigenstructure desired. Following the definition of eigenvalue and eigenvector for the controlled

system, it is possible to write the relationship

$$(\mathbf{A_{cl}} - \lambda_i[\mathbf{I}])\mathbf{\Phi_i} = \underline{\mathbf{0}} \tag{7}$$

for $i = 1 \ldots N$, where N is the dimension of $[\mathbf{A_{cl}}]$, λ_i is the ith eigenvalue and $\mathbf{\Phi_i}$ is the corresponding eigenvector. Since the last two equations are decoupled, the definition of eigenvalue–eigenvector can be written as

$$\begin{bmatrix} a_{11}-\lambda_i & a_{12} & a_{13} & a_{14} \\ a_{21} & a_{22}-\lambda_i & a_{23} & a_{24} \end{bmatrix} \begin{bmatrix} \lambda_i\Phi_{i3} \\ \lambda_i\Phi_{i4} \\ \Phi_{i3} \\ \Phi_{i4} \end{bmatrix} = \begin{bmatrix} 0 \\ 0 \end{bmatrix}. \tag{8}$$

The elements Φ_{i3} and Φ_{i4} represent the components of the ith mode shapes for the two dof system in (figure 1) from a mechanical point of view. The mechanical nature of the problem imposes a structure of the ith eigenvector in state space form and a relation between its first two terms and the final two through the corresponding ith eigenvalue. In the example it is possible to write $N = 4$ times equation (8), obtaining eight equations in eight unknowns. The equations can be rearranged placing the terms a_{ij} in the unknown vector and ordering them in such a way that the final linear system can be written as

$$\begin{bmatrix} \lambda_1\Phi_{13} & \lambda_1\Phi_{14} & \Phi_{13} & \Phi_{14} & 0 & 0 & 0 & 0 \\ \lambda_2\Phi_{23} & \lambda_2\Phi_{24} & \Phi_{23} & \Phi_{24} & 0 & 0 & 0 & 0 \\ \lambda_3\Phi_{33} & \lambda_3\Phi_{34} & \Phi_{33} & \Phi_{34} & 0 & 0 & 0 & 0 \\ \lambda_4\Phi_{43} & \lambda_4\Phi_{44} & \Phi_{43} & \Phi_{44} & 0 & 0 & 0 & 0 \\ 0 & 0 & 0 & 0 & \lambda_1\Phi_{13} & \lambda_1\Phi_{14} & \Phi_{13} & \Phi_{14} \\ 0 & 0 & 0 & 0 & \lambda_2\Phi_{23} & \lambda_2\Phi_{24} & \Phi_{23} & \Phi_{24} \\ 0 & 0 & 0 & 0 & \lambda_3\Phi_{33} & \lambda_3\Phi_{34} & \Phi_{33} & \Phi_{34} \\ 0 & 0 & 0 & 0 & \lambda_4\Phi_{43} & \lambda_4\Phi_{44} & \Phi_{43} & \Phi_{44} \end{bmatrix} \times \begin{bmatrix} a_{11} \\ a_{12} \\ a_{13} \\ a_{14} \\ a_{21} \\ a_{22} \\ a_{23} \\ a_{24} \end{bmatrix} = \begin{bmatrix} \lambda_1^2\Phi_{13} \\ \lambda_2^2\Phi_{23} \\ \lambda_3^2\Phi_{33} \\ \lambda_4^2\Phi_{43} \\ \lambda_1^2\Phi_{14} \\ \lambda_2^2\Phi_{24} \\ \lambda_3^2\Phi_{34} \\ \lambda_4^2\Phi_{44} \end{bmatrix}. \tag{9}$$

The solution of the system allows the control gain matrix to be defined. Note that the coefficient matrix is block diagonal and the blocks are identical.

This method of eigenstructure assignment will be used below to impose real mode shapes and complex conjugate eigenvalues. Note that a real mode shape with a correspondent complex eigenvalue implies a corresponding complex eigenvector in state space formulation. With these assumptions it is possible to prove that the solution of the linear system in equation (9) always exists, is unique and is also real. Thus the gain matrix is real.

2.1. Proof of the existence and uniqueness of a real gain matrix

In this section, eigenstructure assignment in a linear time invariant system, described by equation (2), is proved by assigning complex conjugate pairs of complex eigenvectors and complex eigenvalues using a real control gain matrix.

As mentioned above, $\lambda_2 = \overline{\lambda_1}, \lambda_4 = \overline{\lambda_3}$ where $^-$ is the complex conjugate operator. Furthermore $[\Phi_{23}, \Phi_{24}] = [\overline{\Phi_{13}, \Phi_{14}}]$ and $[\Phi_{43}, \Phi_{44}] = [\overline{\Phi_{33}, \Phi_{34}}]$. The necessary and sufficient condition for ensuring the existence of a unique solution is that the imposed mode shapes be independent and the assigned eigenvalues distinct. These considerations make the coefficient matrix in equation (9) non-singular, which guarantees a unique solution of the linear system. It is important to note that the couples of equations (1) and (2), (3) and (4), . . . , (7) and (8) have a particular structure in that the rows of the coefficient matrix and of the correspondent known vector are complex conjugate. Consider for instance the first block equation

$$\begin{aligned} &\lambda_1\Phi_{13}a_{11} + \lambda_1\Phi_{14}a_{12} + \Phi_{13}a_{13} + \Phi_{14}a_{14} = \lambda_1^2\Phi_{13} \\ &\lambda_2\Phi_{23}a_{11} + \lambda_2\Phi_{24}a_{12} + \Phi_{23}a_{13} + \Phi_{24}a_{14} = \lambda_2^2\Phi_{23} \\ &\lambda_3\Phi_{33}a_{11} + \lambda_3\Phi_{34}a_{12} + \Phi_{33}a_{13} + \Phi_{34}a_{14} = \lambda_3^2\Phi_{33} \\ &\lambda_4\Phi_{43}a_{11} + \lambda_4\Phi_{44}a_{12} + \Phi_{43}a_{13} + \Phi_{44}a_{14} = \lambda_4^2\Phi_{43}. \end{aligned} \tag{10}$$

The known terms are $\lambda_2^2\Phi_{23} = \overline{\lambda_1^2\Phi_{13}}$ and $\lambda_4^2\Phi_{43} = \overline{\lambda_3^2\Phi_{33}}$, thus

$$\begin{aligned} &(\lambda_1\Phi_{13}a_{11} + \lambda_1\Phi_{14}a_{12} + \Phi_{13}a_{13} + \Phi_{14}a_{14}) \\ &\quad = \overline{(\lambda_2\Phi_{23}a_{11} + \lambda_2\Phi_{24}a_{12} + \Phi_{23}a_{13} + \Phi_{24}a_{14})} \\ &(\lambda_3\Phi_{33}a_{11} + \lambda_3\Phi_{34}a_{12} + \Phi_{33}a_{13} + \Phi_{34}a_{14}) \\ &\quad = \overline{(\lambda_4\Phi_{43}a_{11} + \lambda_4\Phi_{44}a_{12} + \Phi_{43}a_{13} + \Phi_{44}a_{14})} \end{aligned} \tag{11}$$

and collecting the unknown terms a_{ij} the result is

$$\begin{aligned} &\lambda_1\Phi_{13}(a_{11} - \overline{a_{11}}) + \lambda_1\Phi_{14}(a_{12} - \overline{a_{12}}) \\ &\quad + \Phi_{13}(a_{13} - \overline{a_{13}}) + \Phi_{14}(a_{14} - \overline{a_{14}}) = 0 \\ &\lambda_3\Phi_{33}(a_{11} - \overline{a_{11}}) + \lambda_3\Phi_{34}(a_{12} - \overline{a_{12}}) \\ &\quad + \Phi_{33}(a_{13} - \overline{a_{13}}) + \Phi_{34}(a_{14} - \overline{a_{14}}) = 0. \end{aligned} \tag{12}$$

The terms in the brackets originating from the difference between two complex conjugate elements are real, as are terms Φ_{i3} and Φ_{i4}. Only the first two members of the sum could be complex. In any case, to satisfy (12) the imaginary part of the sum must be zero and so

$$\begin{aligned} &\lambda_1(\Phi_{13}(a_{11} - \overline{a_{11}}) + \Phi_{14}(a_{12} - \overline{a_{12}})) = c1 \qquad c1 \in \Re \\ &\lambda_3(\Phi_{33}(a_{11} - \overline{a_{11}}) + \Phi_{34}(a_{12} - \overline{a_{12}})) = c2 \qquad c2 \in \Re. \end{aligned} \tag{13}$$

Consider for instance the first relation. Since the terms $\Phi_{13}(a_{11} - \overline{a_{11}})$ and $\Phi_{14}(a_{12} - \overline{a_{12}})$ are real and λ_i is complex, the relation is satisfied if and only if $c1 = 0$. The same holds good for the second equation.

Once it is demonstrated that $c1 = 0$ and $c2 = 0$, the two relations in equation (13) can be satisfied for every pair of

$[\Phi_{13},\ \Phi_{14}]^{\mathrm{T}}$ and $[\Phi_{33},\ \Phi_{34}]^{\mathrm{T}}$ if and only if

$$\begin{aligned}(a_{11} - \overline{a_{11}}) &= 0\\ (a_{12} - \overline{a_{12}}) &= 0.\end{aligned} \tag{14}$$

It follows that in (12), since the sum of the first two terms in each equation is zero, to impose any possible mode shape $[\Phi_{13},\ \Phi_{14}]$ and $[\Phi_{33},\ \Phi_{34}]$, a_{13} and a_{14} must be real. The same conclusions can be drawn for the second block of equations in (9), demonstrating that all the elements a_{ij} are real.

3. Modal space control formulation

Consider now a generic mechanical system made up of discrete or continuous elements. Its dynamics are described by equation (1). Also in the case of continuous systems, the modeling returns discrete matrices (n dofs). These matrices can be obtained from experimental tests or numerically, using, for instance, the finite element method (FEM). Therefore, modal space control can be applied. This technique, classified as a 'model based' control, makes it possible to define the control law from a model in principal coordinates. The change in principal coordinates

$$\underline{\mathbf{z}} = [\Phi]\underline{\mathbf{q}}_{\mathbf{n}} \tag{15}$$

is performed through a transformation matrix $[\Phi] \in \mathbf{R^{n\times n}}$, containing the eigenvectors of $[\mathbf{M}]^{-1}[\mathbf{K}]$ that are the mode shapes of the system. If the structural damping satisfies the Rayleigh assumption, i.e. $[\mathbf{R}] = \alpha[\mathbf{M}] + \beta[\mathbf{K}]$, the transformation matrix $[\Phi]$ is able to diagonalize the matrix differential equation so that each mode evolves independently of the others. The system's equations of motion become

$$[\mathbf{M_q}]\ddot{\underline{\mathbf{q}}}_{\mathbf{n}} + [\mathbf{R_q}]\dot{\underline{\mathbf{q}}}_{\mathbf{n}} + [\mathbf{K_q}]\underline{\mathbf{q}}_{\mathbf{n}} = [\mathbf{B_{qc}}]\underline{\mathbf{F}}_{\mathbf{c}} + [\mathbf{B_{qd}}]\underline{\mathbf{F}}_{\mathbf{d}} \tag{16}$$

where

$$\begin{aligned}[\mathbf{M_q}] &= [\Phi]^{\mathbf{T}}[\mathbf{M}][\Phi]\\ [\mathbf{R_q}] &= [\Phi]^{\mathbf{T}}[\mathbf{R}][\Phi]\\ [\mathbf{K_q}] &= [\Phi]^{\mathbf{T}}[\mathbf{K}][\Phi]\\ [\mathbf{B_{qc}}] &= [\Phi]^{\mathbf{T}}\left[\Lambda_{\mathbf{F_c}}\right]^{\mathbf{T}}\\ [\mathbf{B_{qd}}] &= [\Phi]^{\mathbf{T}}\left[\Lambda_{\mathbf{F_d}}\right]^{\mathbf{T}}.\end{aligned} \tag{17}$$

The matrices $[\mathbf{M_q}]$, $[\mathbf{R_q}]$, $[\mathbf{K_q}]$ are diagonal and $[\mathbf{B_{qc}}]$, $[\mathbf{B_{qd}}]$ are respectively the Lagrangian components of the control and disturbance forces on the principal coordinates. Generally, to reduce the work needed for computation and identification, the modal model is reduced to a set of m modes suitable for reproducing the system's dynamics in the frequency range desired. As discussed above, different control techniques have been developed starting from the modal approach.

3.1. Independent modal space control

In independent modal space control (IMSC), the control matrices are computed so that the controlled modes have the desired damping ratio and natural frequency acting independently on each of the decoupled differential equations. Assuming that the dimension of the reduced control model is m, it is possible to partition equation (16) into two subsystems, of dimensions m and $(n - m)$ respectively, as

$$\begin{aligned}&[\mathbf{M_{qm}}]\ddot{\underline{\mathbf{q}}}_{\mathbf{m}} + [\mathbf{R_{qm}}]\dot{\underline{\mathbf{q}}}_{\mathbf{m}} + [\mathbf{K_{qm}}]\underline{\mathbf{q}}_{\mathbf{m}}\\ &\quad = [\mathbf{B_{qcm}}]\underline{\mathbf{F}}_{\mathbf{c}} + [\mathbf{B_{qdm}}]\underline{\mathbf{F}}_{\mathbf{d}}\\ &[\mathbf{M_{qnm}}]\ddot{\underline{\mathbf{q}}}_{\mathbf{nm}} + [\mathbf{R_{qnm}}]\dot{\underline{\mathbf{q}}}_{\mathbf{nm}} + [\mathbf{K_{qnm}}]\underline{\mathbf{q}}_{\mathbf{nm}}\\ &\quad = [\mathbf{B_{qcnm}}]\underline{\mathbf{F}}_{\mathbf{c}} + [\mathbf{B_{qdnm}}]\underline{\mathbf{F}}_{\mathbf{d}}.\end{aligned} \tag{18}$$

The control force is computed as

$$\underline{\mathbf{F}}_{\mathbf{c}} = [\mathbf{B_{qcm}}]^{-1}([\mathbf{G_v}]\dot{\underline{\mathbf{q}}}_{\mathbf{m}} + [\mathbf{G_p}]\underline{\mathbf{q}}_{\mathbf{m}}) \tag{19}$$

where the matrices $[\mathbf{G_v}]$ and $[\mathbf{G_p}]$ are diagonal in order to keep the modes decoupled and thus not modify the system mode shapes. Applying the control law to the full model, equation (18) becomes

$$[\mathbf{M_{qc}}]\ddot{\underline{\mathbf{q}}}_{\mathbf{n}} + [\mathbf{R_{qc}}]\dot{\underline{\mathbf{q}}}_{\mathbf{n}} + [\mathbf{K_{qc}}]\underline{\mathbf{q}}_{\mathbf{n}} = [\mathbf{B_{qd}}]\underline{\mathbf{F}}_{\mathbf{d}} \tag{20}$$

where

$$\begin{aligned}[\mathbf{M_{qc}}] &= \begin{bmatrix}\mathbf{M_{qm}} & [\mathbf{0}]\\ [\mathbf{0}] & \mathbf{M_{qnm}}\end{bmatrix}\\ [\mathbf{R_{qc}}] &= \begin{bmatrix}\mathbf{R_{qm}} - \mathbf{G_v} & [\mathbf{0}]\\ -\mathbf{B_{qcnm}}\mathbf{B_{qcm}^{-1}}\mathbf{G_v} & \mathbf{R_{qnm}}\end{bmatrix}\\ [\mathbf{K_{qc}}] &= \begin{bmatrix}\mathbf{K_{qm}} - \mathbf{G_p} & [\mathbf{0}]\\ -\mathbf{B_{qcnm}}\mathbf{B_{qcm}^{-1}}\mathbf{G_p} & \mathbf{K_{qnm}}\end{bmatrix}\\ [\mathbf{B_{qd}}] &= \begin{bmatrix}\mathbf{B_{qdm}}\\ \mathbf{B_{qdnm}}\end{bmatrix}.\end{aligned} \tag{21}$$

Control spillover due to the non-diagonal entries in the damping and stiffness controlled matrices can be highlighted. Moreover, looking at the structure of the closed loop system dynamics, the presence of the extra-diagonal terms will couple the non-controlled principal coordinates with the controlled coordinates.

4. Dependent modal space control

Based on the above considerations, the control strategy proposed in this paper uses the extra-diagonal entries of the matrices $[\mathbf{G_v}]$ and $[\mathbf{G_p}]$ that become full gain matrices (dependent modal space control, DMSC). These entries can be used in two different ways.

- Direct imposition: definition of mode shapes in a finite number of m system dofs.
- Indirect imposition: optimal mode shapes minimizing a desired performance index.

4.1. Eigenvector assignment through DMSC

To assign the eigenvectors and eigenvalues using modal control, the theorem presented in section 2 is used on the reduced control model in principal coordinates. The first

equation of (18) can be rewritten in state space formulation as

$$\dot{\underline{\mathbf{x}}}_{\mathbf{qm}} = [\mathbf{A_{qm}}]\underline{\mathbf{x}}_{\mathbf{qm}} + [\mathbf{B_{xqcm}}]\underline{\mathbf{F}}_{\mathbf{c}} + [\mathbf{B_{xqdm}}]\underline{\mathbf{F}}_{\mathbf{d}} \tag{22}$$

where

$$\underline{\mathbf{x}}_{\mathbf{qm}} = \begin{bmatrix} \dot{\underline{\mathbf{q}}}_{\mathbf{m}} \\ \underline{\mathbf{q}}_{\mathbf{m}} \end{bmatrix}$$
$$[\mathbf{B_{xqcm}}] = \begin{bmatrix} [\mathbf{B_{qcm}}] \\ [\mathbf{0}] \end{bmatrix} \tag{23}$$
$$[\mathbf{B_{xqdm}}] = \begin{bmatrix} [\mathbf{B_{qdm}}] \\ [\mathbf{0}] \end{bmatrix}.$$

Finally the closed loop matrix results,

$$[\mathbf{A_{qmcl}}] = [[\mathbf{A_{qm}}] + [\mathbf{B_{xqcm}}][\mathbf{B_{qcm}}]^{-1}[[\mathbf{G_v}]\,[\mathbf{G_p}]]]. \tag{24}$$

Note that

$$[\mathbf{G}] = [\mathbf{B_{qcm}}]^{-1}[[\mathbf{G_v}]\,[\mathbf{G_p}]] \tag{25}$$

and the split of the control gain matrix into two sub-matrices serves simply to underline the entries of [**G**] that multiply the modal velocities by the ones that multiply the modal displacement.

Assigning the $[\mathbf{A_{qmcl}}]$ eigenvalues allows the desired damping ratio and frequencies of the controlled modes to be selected, while $[\mathbf{A_{qmcl}}]$ eigenvector assignment determines a combination of the open loop uncoupled mode shapes. Consider, for example, that three modes have to be controlled ($m = 3$); denote the ith controlled mode shape in correspondence of three physical coordinates as (Φ_{Cia}, Φ_{Cib}, Φ_{Cic}). It is possible to write the relation

$$\begin{bmatrix} \Phi_{Cia} \\ \Phi_{Cib} \\ \Phi_{Cic} \end{bmatrix} = \begin{bmatrix} \Phi_{1a} \\ \Phi_{1b} \\ \Phi_{1c} \end{bmatrix} w_{i1} + \begin{bmatrix} \Phi_{2a} \\ \Phi_{2b} \\ \Phi_{2c} \end{bmatrix} w_{i2} + \begin{bmatrix} \Phi_{3a} \\ \Phi_{3b} \\ \Phi_{3c} \end{bmatrix} w_{i3} \tag{26}$$

where a linear combination of the uncontrolled mode shapes in the selected physical coordinates are suitably weighted in order to obtain the desired closed loop mode shape. Writing the same equations also for the remaining two mode shapes, we can obtain

$$\begin{bmatrix} \Phi_{C1a} & \Phi_{C2a} & \Phi_{C3a} \\ \Phi_{C1b} & \Phi_{C2b} & \Phi_{C3b} \\ \Phi_{C1c} & \Phi_{C2c} & \Phi_{C3c} \end{bmatrix} = \begin{bmatrix} \Phi_{1a} & \Phi_{2a} & \Phi_{3a} \\ \Phi_{1b} & \Phi_{2b} & \Phi_{3b} \\ \Phi_{1c} & \Phi_{2c} & \Phi_{3c} \end{bmatrix} \begin{bmatrix} w_{11} & w_{21} & w_{31} \\ w_{12} & w_{22} & w_{32} \\ w_{13} & w_{23} & w_{33} \end{bmatrix}. \tag{27}$$

In a more compact way

$$[\mathbf{\Phi_C}] = [\mathbf{\Phi_{abc}}][\mathbf{W}]. \tag{28}$$

Once the desired discrete closed loop mode shapes $[\mathbf{\Phi_C}]$ are selected, with the corresponding uncontrolled mode shapes $[\mathbf{\Phi_{abc}}]$ known, it is possible to compute the weighting matrix coefficient [**W**] that represents the controlled mode shapes of the system described in principal coordinates. Finally, assembling the desired closed loop poles with [**W**], it is possible to compute the eigenvectors of the closed loop system in principal coordinates in state space formulation and thus the corresponding dynamic matrix $[\mathbf{A_{qmcl}}]$ as explained in section 2. Once the dynamic matrices respectively in open $[\mathbf{A_{qm}}]$ and closed loop $[\mathbf{A_{qmcl}}]$ and the input matrix $[\mathbf{B_{xqcm}}]$ are known, it is possible to compute the control gain matrix [**G**] and its subcomponents through equations (24) and (25). Note that IMSC is a particular case of the DMSC where the [**W**] coefficient matrix in equation (27) is an identity, leaving the mode shapes unaltered. The conditions required to ensure the existence of a unique solution mentioned in section 2 have to be taken into account in the selection of the Φ_{Cij} values. In equation (27), the matrix $[\mathbf{\Phi_{abc}}]$, as a subset of [**Φ**], may always be inverted because of the orthogonal propriety of the mode shapes. To ensure that [**W**] is non-singular, the matrix $[\mathbf{\Phi_C}]$ has to be non-singular. Even if the exact modal coordinates are available for control (by using for example a modal sensor), the closed loop system described in equations (20) and (21) shows extra-diagonal terms due only to control spillover, which couple the non-controlled modes with the controlled ones. In this way the uncontrolled modes affect the first m modes and the mode shape imposition in the desired dof is not possible. The use of DMSC with the direct assignment of the closed loop eigenvectors requires modal sensors and modal actuators in order to be effective.

4.2. Performance index minimization through DMSC

In many applications of vibration reduction for continuous systems, the availability of sensors and actuators is limited, and also their positions cannot always be chosen by the control designer. In this section we show how the use of DMSC makes it possible to take advantage of the full gain matrices and the possibility of modifying the mode shapes as well as the system poles. The proposed control strategy is particularly useful for suppressing vibrations at desired points of the structure and in a determined range of frequencies. The integral of FRF amplitude between the disturbance and the displacement of a desired point where vibration suppression is required is chosen as the performance index to be minimized,

$$\mathrm{PI} = \int_{\Omega_{\min}}^{\Omega_{\max}} |\mathrm{FDT}|_{F_{\mathrm{d}^- > Y}}\, \mathrm{d}\Omega. \tag{29}$$

Since the selected performance index is an input–output relation, the position of the disturbance action or its Lagrangian components must be either known or estimated [5]. As mentioned in the introduction, the FRF absolute value is considered disregarding the phase, since the stability check is included in the optimization. If vibration needs to be suppressed at more than one point, the performance index is a weighted sum of the individual ones. The optimal closed loop mode shapes are selected using a genetic algorithm (GA, [13, 14]) performing a constrained optimization. In order to avoid a local minimum and ensure the convergence of the GA, the gain matrix [**G**] has been computed by using different initial populations and by leading it to converge to

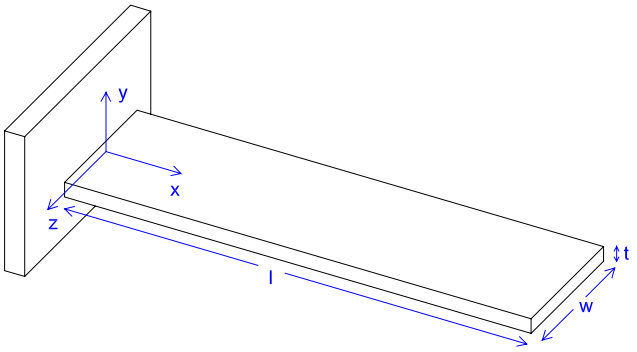

Figure 2. The cantilever beam: main dimensions and reference system.

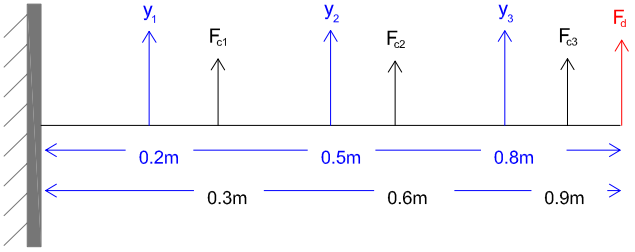

Figure 3. The cantilever beam: positions of sensors, actuators and disturbance force.

Table 1. The cantilever beam main characteristics.

l (m)	w (m)	t (mm)	E (MPa)	m (kg m^{-1})
1	0.04	6.1	75 000	0.754

Table 2. The cantilever beam model parameters (ω and ξ) for the first eight modes.

Mode no	1	2	3	4	5	6	7	8
f (Hz)	5.3	33	92.4	181.2	300	448	625.4	833
ξ (%)	0.42	0.13	0.2	0.36	0.58	0.86	1.2	1.6

the same reliable solution. The computational cost for the proposed optimization scheme is very low with a running time shorter than 1 min on a standard notebook (CPU Intel(R) Core(TM) i7 and 8 GB RAM). The frequency range $[\Omega_{\min}, \Omega_{\max}]$ is selected according to the kind of disturbance exciting the structure and is strictly related to the physical application. The optimization procedure considers a reduced model of the system of order p, which is in general different from m. The parameter p is selected realizing a trade-off between the accuracy of the performance index, the stability conditions of the closed loop and the work needed in identifying the parameters. Therefore, performing the constrained optimization with a model of order p while controlling the first m modes, the closed loop stability of the first p modes is ensured.

The choice of the parameter p is pivotal and it is strictly related to the structure's dynamics and the designer's experience. However, the first uncontrolled $p - m$ modes are generally the most critical and sensitive to instability due to spillover effects. The higher ones, indeed, respond in the quasi-static region and they have a higher structural damping increasing with the frequency.

The stability constraint assures that the real part of the first p closed loop poles is strictly lower than zero. In any case it should be noted that it is also possible to impose a minimum threshold damping for the closed loop poles to guarantee a desired stability margin.

The application of DMSC in this latter way can be summarized in five steps.

- Selection of the frequency range in which the index should be minimized, [$\Omega_{\min}$ and $\Omega_{\max}$].
- Selection of the desired controlled poles m of the system in terms of damping ratio ξ and frequency ω.
- Selection of the number of modes p considered in the algorithm on which the stability of the closed loop is ensured.
- The optimal set of closed loop mode shapes found by the GA such that the performance index is minimal given the stability constraints.
- Calculation of the matrices $[\mathbf{G_v}]$ and $[\mathbf{G_p}]$.

5. Numerical analysis

A numerical model using the FEM approach describing the dynamics of an aluminum beam clamped in the vertical plane (figure 2) is used to test the logics proposed. The system has 21 nodes (one constrained) with three dofs per node (axial and transversal displacement and bending rotation), resulting in a total of $n = 60$ dofs. The characteristics of the clamped beam are shown in table 1.

Three pairs of non-collocated sensors and actuators are used to control the first three modes ($m = 3$) and the respective locations are shown in figure 3, as well as the unknown disturbance F_{d}. The frequencies and the damping ratio of the system's first eight modes are shown in table 2.

The two DMSC versions described in section 4 are analyzed.

First, the numerical results of what was explained in section 4.1 are reported; the controlled poles are selected so that their damping ratio is equal to 0.15 and the controlled frequencies are equal to the non-controlled ones (for both IMSC and DMSC). Figure 4 shows the uncontrolled versus the controlled modes; the markers indicate the imposed values of $\Phi_{Ci,j}$. Figure 5 presents the FRF between F_{d} and the three outputs $Y_{a,b,c}$ and the three control forces. Note in each figure the presence of a single resonance peak for the first three eigenfrequencies, due to the creation of virtual nodes, and a consequent increase of control forces. A time domain analysis is also carried out. In particular, the impulse response is shown in figure 6 to emphasize the performance of the DMSC compared with the IMSC in a wide frequency range.

Similarly, the numerical results when the DMSC is used to minimize the performance index, as explained in section 4.2, are reported. They will be presented both in

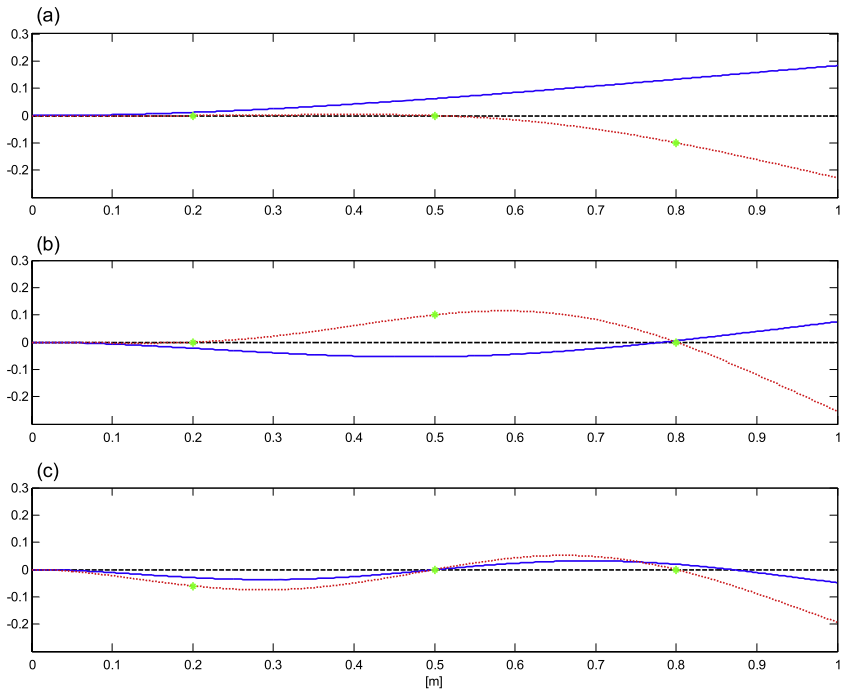

Figure 4. DMSC eigenvector assignment: original (continuous line) and imposed (dotted line) mode shapes (star markers); mode 1 at 5.27 Hz (a), mode 2 at 33.02 Hz (b), mode 3 at 92.46 Hz (c).

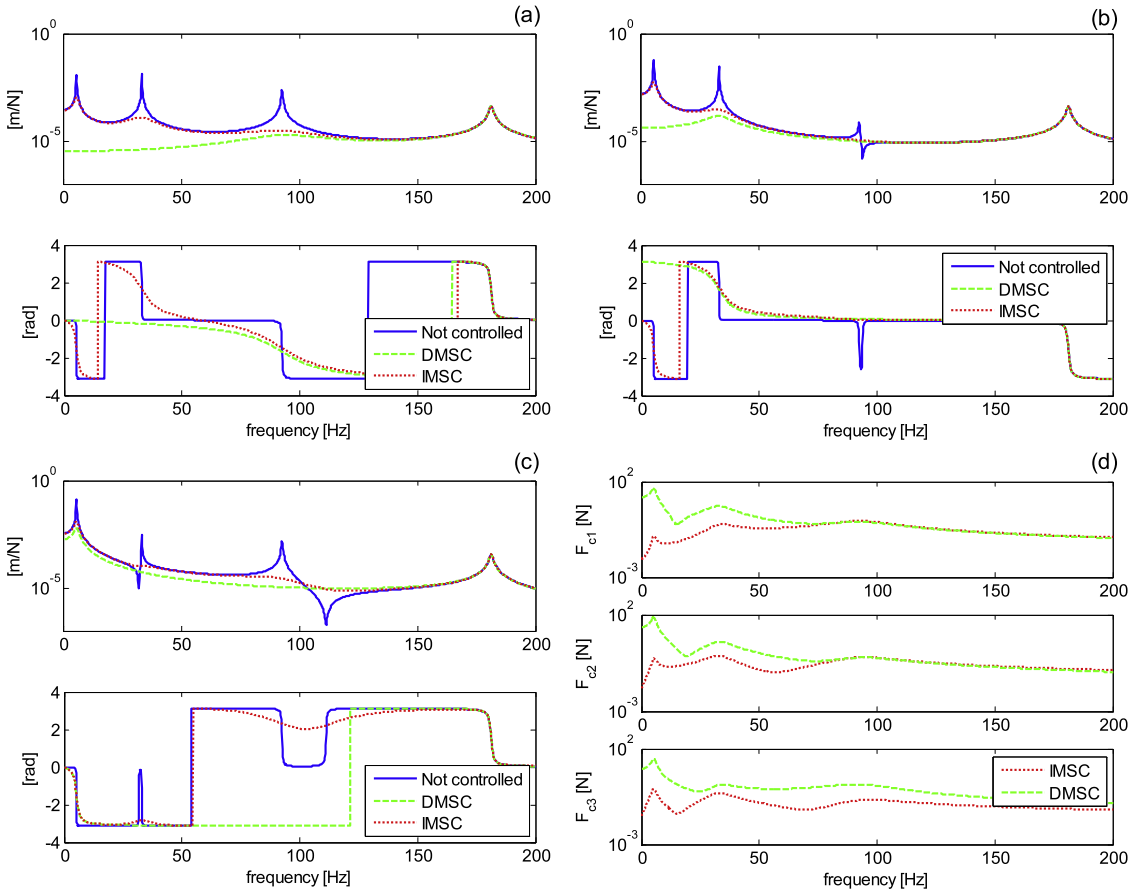

Figure 5. DMSC eigenvector assignment: FRF between the disturbance F_{d} and the output Y_a (a), Y_b (b), Y_c (c) and the three control forces (d).

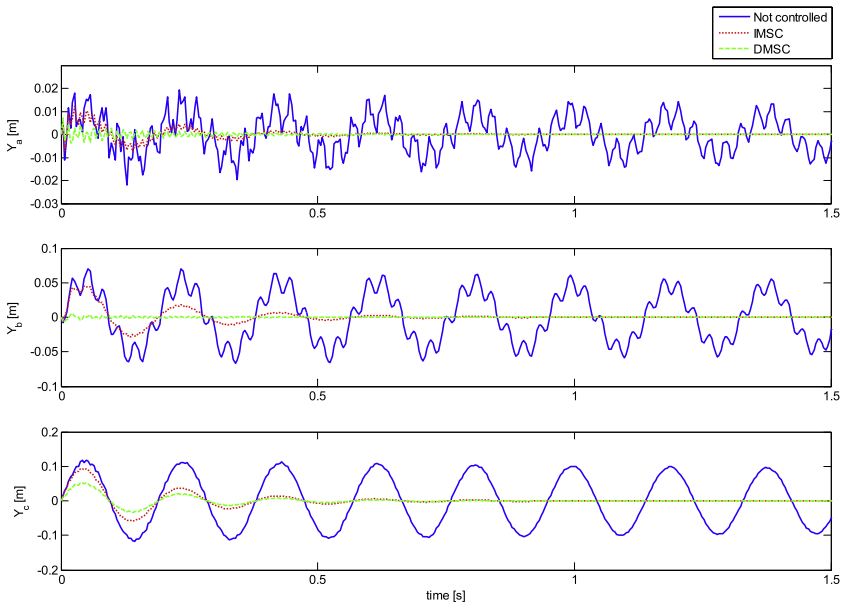

Figure 6. DMSC eigenvector assignment: response to impulse disturbance time history at the measurement points for no control, IMSC and DMSC.

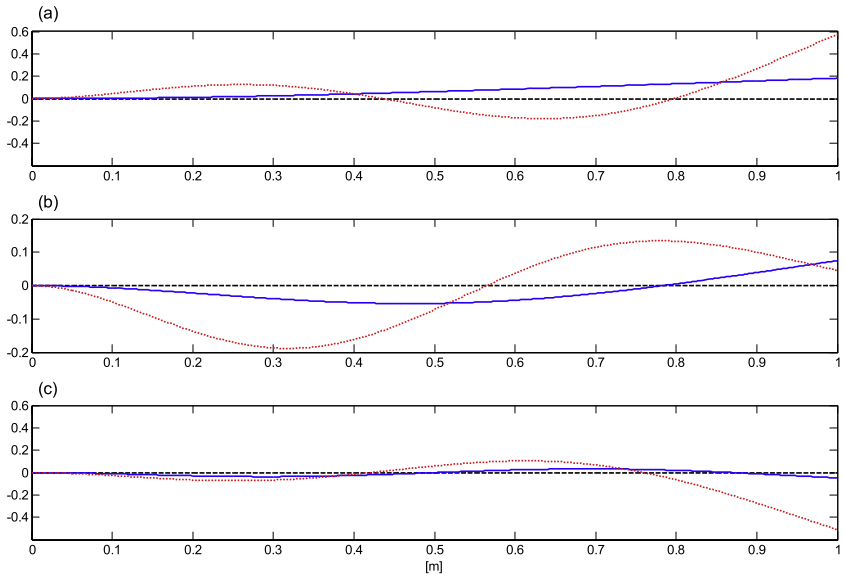

Figure 7. DMSC performance index minimization: original (continuous line) and optimal (dotted line) mode shapes (when the modal coordinates are directly measured); mode 1 at 5.27 Hz (a), mode 2 at 33.02 Hz (b), mode 3 at 92.46 Hz (c).

the case where the exact principal coordinates are available for control (e.g. by using distributed sensors) and in the case where they are estimated through a dynamic observer. The selected controlled poles are chosen as in the previous example. In this case, p (the number of modes involved in the performance index minimization) was 8, for the reasons explained in section 4.2; the selected frequency range of optimization is [0–200] Hz.

In the case of distributed sensors, the optimal set of controlled mode shapes returned by the minimization algorithm is shown in figure 7. Figure 8 shows respectively the FRF between F_{d} and the three measures $Y_{a,b,c}$ and the three control forces. Finally, figure 9 shows the time response to a random disturbance with frequency content up to 200 Hz. These results highlight the performance of the DMSC with respect to the IMSC. In this case improvement is possible with a limited increase of control forces. The calculation of time history RMS shows an average reduction of 80% comparing no control with IMSC, and almost 100% when comparing no control with DMSC.

When a dynamic observer is used to estimate the principal coordinates, the order of the observer model m_{o} is set to 6, while only the first three estimated coordinates are used for control (as in the previous cases). The observer poles are selected so that the damping ratio is equal to 0.3 while the corresponding frequencies are unaltered with respect to the

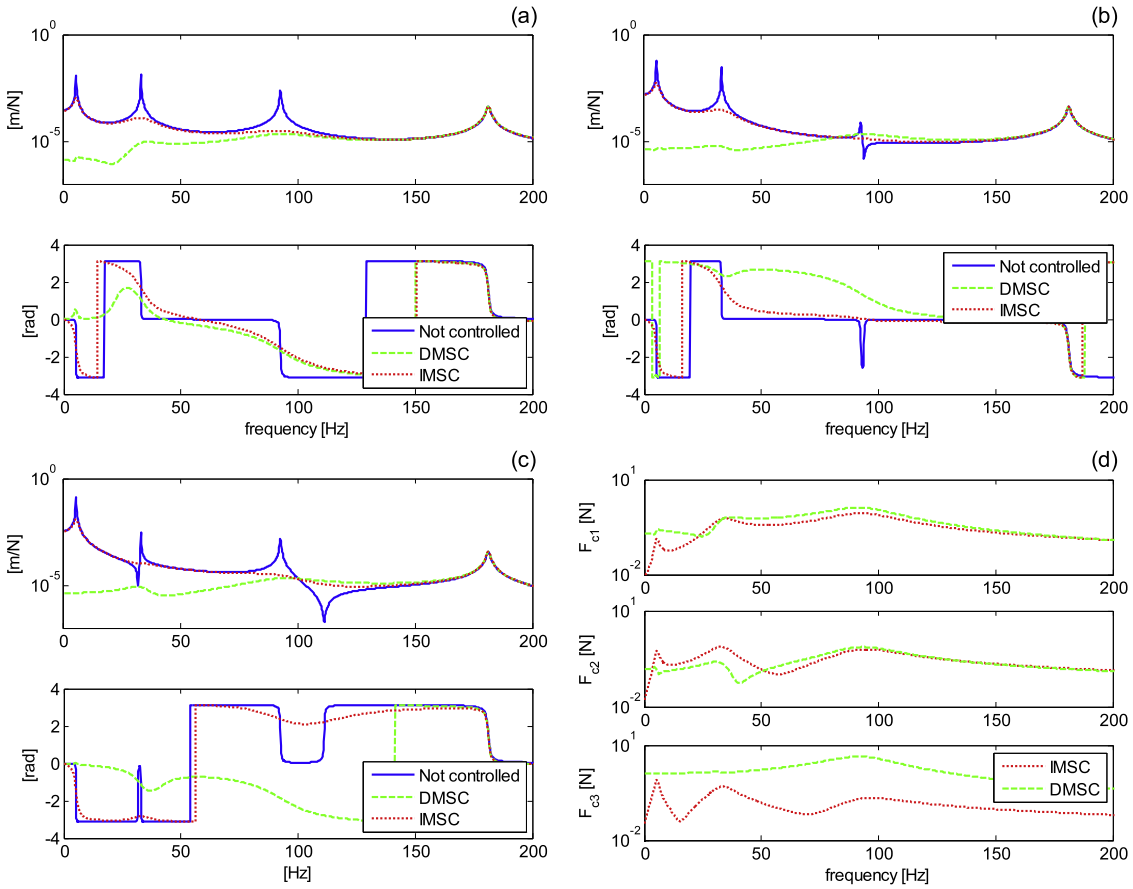

Figure 8. DMSC performance index minimization: FRF between the disturbance F_d and the output Y_a (a), Y_b (b), Y_c (c) and the three control forces (d) (when the modal coordinates are directly measured).

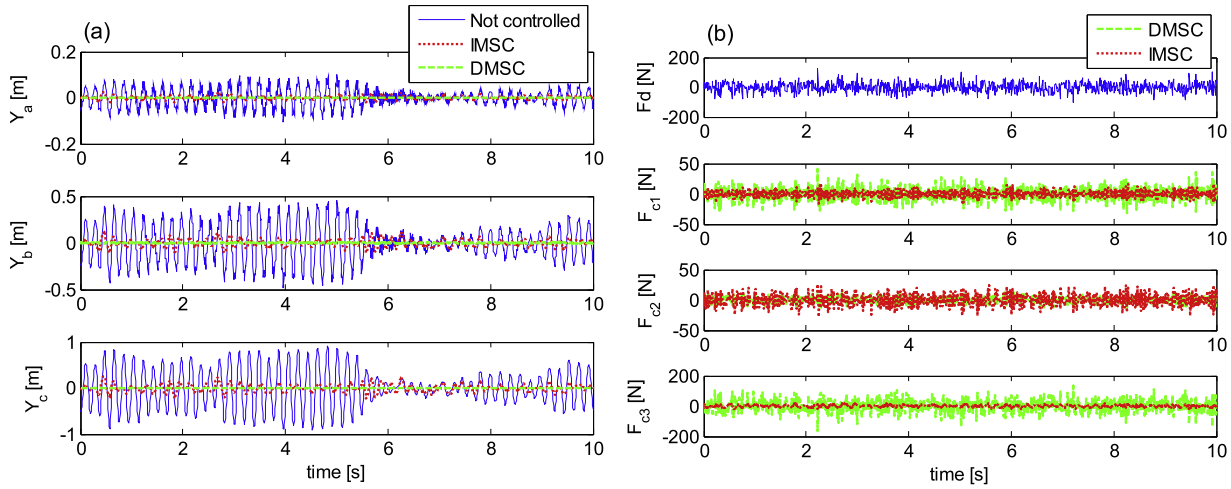

Figure 9. DMSC performance index minimization: response to random disturbance time history in the measurement points (a) and corresponding disturbance and control forces (b) for the non-controlled, IMSC and DMSC (when the modal coordinates are directly measured).

uncontrolled system. The measures available for the dynamic observer are the transverse velocities at the points where the sensors are placed. Figure 10 shows the optimal controlled mode shapes while figures 11 and 12 plot respectively the FRF and the response to a random disturbance force. It is important to note that, for velocity measurements, DMSC chooses the mode shapes in such a way that, unlike earlier methods, the static gains of the FRF are not modified. Also in this case, where no distributed sensors and actuators are available, the performance of DMSC is better than that of IMSC, demonstrating the effectiveness of the control logic. The time responses to the random disturbance show an average RMS reduction of 73% and 89% respectively for IMSC and DMSC, both compared with the non-controlled system.

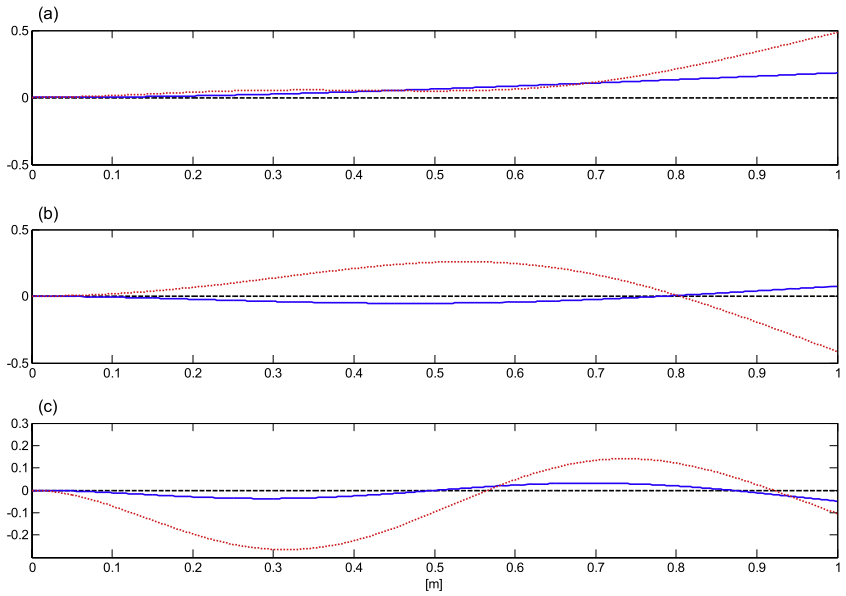

Figure 10. DMSC performance index minimization: original (continuous line) and optimal (dotted line) mode shapes (when the modal coordinates are estimated); mode 1 at 5.27 Hz (a), mode 2 at 33.02 Hz (b), mode 3 at 92.46 Hz (c).

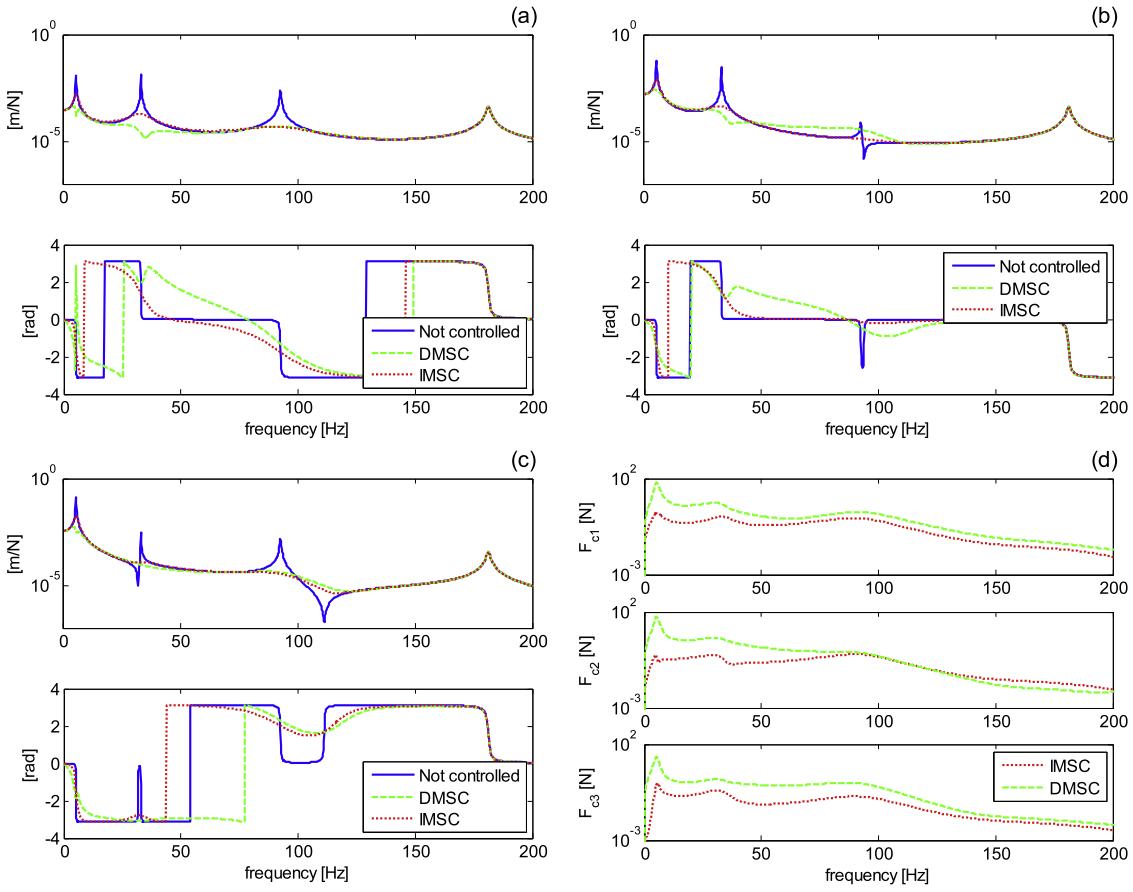

Figure 11. DMSC performance index minimization: FRF between the disturbance F_{d} and the output Y_a (a), Y_b (b), Y_c (c) and the three control forces (d) (when the modal coordinates are estimated).

6. Conclusions

This paper has presented a control strategy based on a modal approach called dependent modal space control (DMSC). Besides the assignment of the controlled poles, the imposition of the controlled mode shapes at a discrete number of points allows virtual nodes to be obtained and provides better performance when DMSC is used to optimize a given index. A main difference between this method and IMSC is the possibility of computing a control law that focuses on

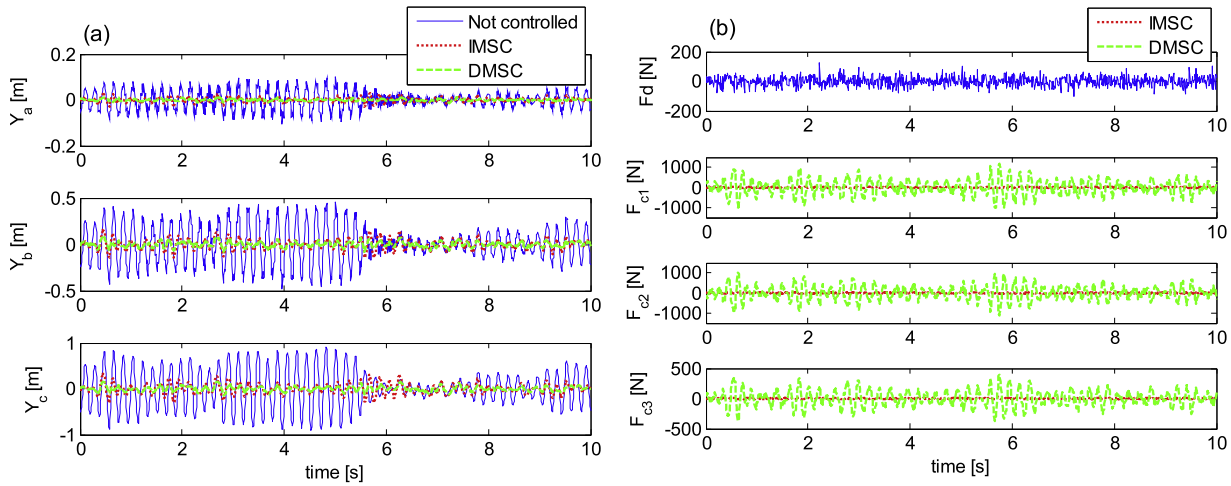

Figure 12. DMSC performance index minimization: response to random disturbance time history in the measurement points (a) and corresponding disturbance and control forces (b) for no control, IMSC and DMSC (when the modal coordinates are estimated).

vibration reduction at desired points and in a desired range of frequencies, while ensuring closed loop stability for a set number of modes. The method proposed was tested in numerical simulations on an FEM model of a cantilever beam and showed the advantages of DMSC over the classic IMSC. However, modification of the mode shapes means that the control forces required by DMSC are generally higher than those needed in IMSC. When the control actuators are not able to implement these forces, they can be reduced by inserting a penalty term in the performance index.

References

[1] Balas M J 1978 Active control of flexible systems *J. Optim. Theory Appl.* **25** 415–36

[2] Meirovitch L 1983 Comparison of control techniques for large flexible systems *J. Guid. Control Dyn.* **6** 302–10

[3] Meirovitch L and Baruh H 1985 Implementation of modal filters for control of structures *J. Guid. Control Dyn.* **8** 707–16

[4] Resta F, Ripamonti F, Cazzulani G and Ferrari M 2010 Independent modal control for nonlinear flexible structures: an experimental test rig *J. Sound Vib.* **329** 961–72

[5] Bagordo G, Cazzulani G, Resta F and Ripamonti F 2011 A modal disturbance estimator for vibration suppression in nonlinear flexible structures *J. Sound Vib.* **330** 6061–9

[6] Baz A and Poh S 1990 Experimental implementation of the modified independent modal space control method *J. Sound Vib.* **139** 133–49

[7] Fang J Q, Li Q S and Jeary A P 2003 Modified independent modal space control of *m* dof systems *J. Sound Vib.* **261** 421–41

[8] Singh S P, Pruthi H S and Agarwal V P 2003 Efficient modal control strategies for active control of vibrations *J. Sound Vib.* **262** 563–75

[9] Kim M H and Inman D J 2001 Reduction of observation spillover in vibration suppression using a sliding mode observer *J. Vib. Control* **7** 1087–105

[10] Mottersheada J E, Tehrania M G, James S and Ram Y M 2008 Active vibration suppression by pole-zero placement using measured receptances *J. Sound Vib.* **311** 1391–408

[11] Liu G P and Patton R J 1998 Low sensitive and robust control design via output feedback *UKACC Int. Conf.* vol 1 p 457

[12] Youn M and Arnold M 1987 Eigenvalue-generalized eigenvector assignment *IEEE Trans. Autom. Control* **32** 417–21

[13] Deep K, Singh K P, Kansal M L and Mohan C 2009 A real coded genetic algorithm for solving integer and mixed integer optimization problems *Appl. Math. Comput.* **212** 505–18

[14] Schmitt L M 2001 Theory of genetic algorithms *Theor. Comput. Sci.* **259** 1–61